

The Experimental Determination of Bearings Dynamic Coefficients in a Wide Range of Rotational Speeds, Taking into Account the Resonance and Hydrodynamic Instability



Łukasz Breńkacz, Grzegorz Żywica, Marta Drosińska-Komor and Natalia Szewczuk-Krypa

Abstract Methods for the experimental determination of dynamic coefficients are commonly used for the analysis of various types of bearings, including hydrodynamic, aerodynamic and foil bearings. There are currently several algorithms that allow estimating bearing dynamic coefficients. Such algorithms usually use various excitation techniques applied to rotor–bearings systems. So far only a small number of scientific publications show how calculated dynamic coefficients of bearings change as speed rises. In the literature, there are no computation results that demonstrate changes in these coefficients either in a broad range of speeds (that would cover resonant speeds) or at speeds at which a phenomenon of hydrodynamic instability can be observed. This article fills the literature gap in question. For calculation purposes, the impulse response method based on an in-house algorithm (with a linear approximation using the least squares method) was applied. On its basis, the stiffness, damping and mass coefficients of a rotor–bearings system were calculated. It turns out that some of the obtained values of damping coefficients are negative at the resonant speed. Moreover, if the values are calculated at a speed at which the

Ł. Breńkacz (✉) · G. Żywica

The Department of Turbine Dynamics and Diagnostics, Institute of Fluid Flow Machinery, Polish Academy of Sciences, Fiszerza 14, 80-231 Gdańsk, Poland
e-mail: lukasz.brenkacz@imp.gda.pl

G. Żywica

e-mail: grzegorz.zywica@imp.gda.pl

M. Drosińska-Komor · N. Szewczuk-Krypa

Faculty of Ocean Engineering and Ship Technology, Gdańsk University of Technology, G. Narutowicza 11/12, 80-233 Gdańsk, Poland
e-mail: mardrosi@pg.edu.pl

N. Szewczuk-Krypa

e-mail: natszewel@pg.edu.pl

hydrodynamic instability phenomenon is present they are accompanied by considerably higher standard deviations. On the basis of our computation results and the literature review, capabilities and limitations of the method used for the experimental identification of dynamic coefficients of hydrodynamic bearings were discussed.

Keywords Bearing dynamic coefficients · Experimental research · Nonlinear coefficients · Impact excitation · Hydrodynamic bearing

1 Introduction

Hydrodynamic radial bearings are commonly used in supporting rotors of power turbines because they allow a long-term operation at very low vibration levels bearings. The literature is rich in articles on the determination of bearings' dynamic coefficients. A review of the articles on this subject is contained in the article [1]. This review also demonstrates how big the measurement errors are. The various approaches to the bearing identification problem are discussed, including the different force excitation methods of incremental loading, sinusoidal, pseudorandom, impulse, known/additional unbalance, and non-contact excitation. Also bearing excitation and rotor excitation approaches are discussed. Data processing methods in the time and frequency domains are presented. Methods of evaluating the effects of measurement uncertainty on overall bearing coefficient confidence levels are reviewed. In this review, the relative strengths and weaknesses of bearing identification methods are presented, and developments and trends in improving bearing measurements are documented. A strong side of this article is the fact that it provides the calculation results of dynamic coefficients of hydrodynamic bearings as a function of the rotational speed. As it turns out, error values generated during calculations vary greatly in a wide range of rotational speeds that covers resonant speeds and higher speeds.

Rotordynamic coefficients of a controllable floating ring bearing (FRB) were measured and described in the article [2]. Controllability of the bearing was achieved by using a magnetorheological fluid (MRF) as a lubricant along with the external magnetic field. Magnetic field induced field-dependent viscosity of the MRF changes dynamic coefficients (stiffness, damping, etc.) of the bearing, and vibration amplitudes of the rotor were suppressed by the enhanced stiffness and/or damping. The rotating floating ring in the FRB separates the MRF into two lubricant films. Since the ring rotates slower than the shaft, shear rate in the outer film is lower compared to the inner film, pertaining controllability by limiting the so-called shear-thinning effect of the MRF. A test rig is built to measure and identify the rotordynamic coefficients of the MRF lubricated FRB. Coefficients of the bearing with various magnetic field strength are compared. Results show enhancements of dynamic properties of the bearing with external magnetic field, demonstrating the viability of this type of smart bearings in rotor control or behaviour alteration applications.

The requirement of bearing coefficients identification based on flexible rotor-bearing systems has stimulated the investigation of bearing forces over the years,

whereby in industry high-speed balancing machines and flexible rotor-bearing test rigs can be used to measure the dynamic force coefficients of bearings [3]. However, the actual rotor vibration at the bearing nodes cannot be measured or simply calculated by the data acquired from a single measurement station outside of the bearing. To solve this problem, a double-section interpolation-iteration method to identify the dynamic coefficients has been developed which uses previously identified coefficients to predict new vibration vectors from a finite element model and then updates the vibration vectors at the bearings to recalculate the coefficients. Moreover, the experimental work, in which an active magnetic bearing was used to excite a flexible test rig supported by tilting pad bearings, was also carried out to validate the method, with the vibration shape predicted by the identified results matching the test data very well and the first forward mode parameters also matching the results from sine-swept identification.

The method for the determination of bearing dynamic coefficients applied by the authors of this article operates in the frequency domain. Its first version was presented by Nordmann and Schoellhorn [4]. The basic algorithm was extended by adding the possibility to compute sixteen stiffness and damping coefficients [5].

In the article [6], an in-house algorithm was used to obtain the dynamic coefficients of bearings. It is a modified version of the algorithm for the computation of stiffness and damping coefficients introduced by Qiu and Tieu. The modification was done in such a manner that it also allows calculating eight mass coefficients. The determination of stiffness, damping and mass coefficients by means of a single algorithm permits verification of the results already in a preliminary stage of an experimental investigation. The identified dynamic coefficients of a bearing can be verified on the basis of mass coefficients since a shaft mass is usually known in advance. This approach allows identifying all dynamical parameters of a rotor—bearings system by means of an experimental research [7]. Some issues connected with the identification of bearing dynamic coefficients and bearing modelling are presented in publications [8–10].

2 Basic Technical Characteristics of the Test Rig

The description of the test rig and research apparatus used during the research can be found in the papers [11, 12]. Figure 1 shows a photo of the test rig, while Fig. 2 contains a diagram illustrating its most important components along with their dimensions. The length of the test rig is 1.25 m, and its width and height are 0.36 and 0.65 m, respectively. The axes of the coordinate system used during the experimental investigation are shown in the top left-hand corner of Fig. 2. The test rig rests on a 13 mm thick steel plate with two channel bars attached to it. The channel bars are equipped with rubber feet (allowing for height adjustment and leveling of the plate). The rotor shaft is supported by two bearings. The system is driven by a three-phase motor with a maximum speed of 3450 rpm. The motor rotations were adjusted by means of a frequency inverter with a capacity of 1.5 kW. The motor is mounted to

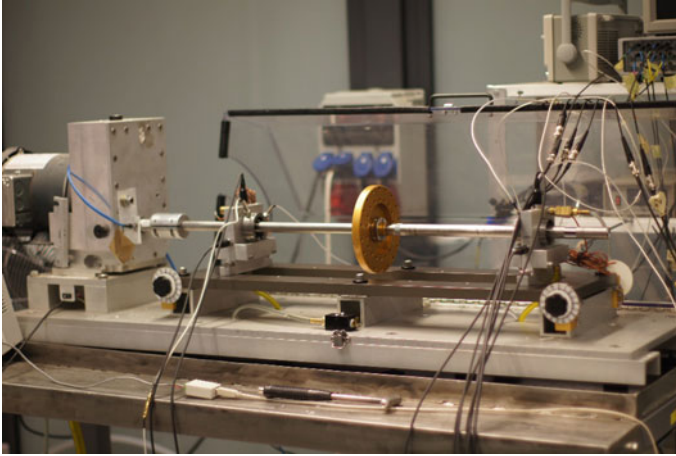


Fig. 1 Photo of the test rig

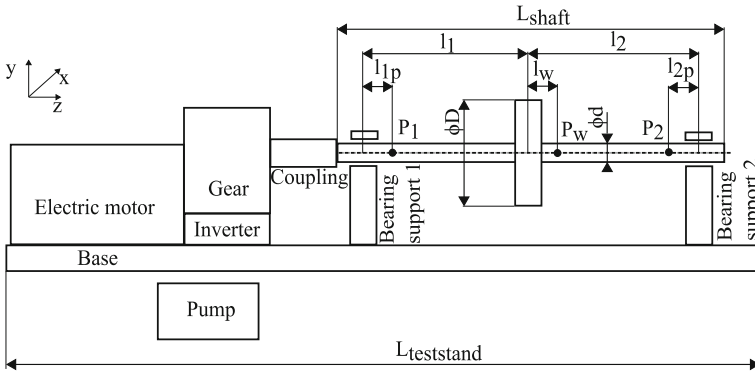


Fig. 2 Diagram of the test rig

a gear that increases the speed with a gear ratio 3.5:1. The presence of the inverter allows varying the motor speed up to 12,000 rpm. The gear is connected to the rotor shaft by means of a permanent coupling. The coupling diameter is 50 mm and its length is 60 mm. The oil lubricated bearing system is equipped with a pump. During experimental tests, the oil pressure was 0.16 MPa.

The tested rotor has a length of 920 mm. The distance between the coupling and the first bearing support is 170 mm. The rotor was mounted in two bearing supports. The distance between the supports is 580 mm. The rotor disc is equidistant to each bearing support. The rotor diameter is 19.02 mm and the rotor disc diameter is 152.4 mm. Excitations were applied to the shaft using an impact hammer at the point that is shifted 30 mm from the rotor disc's midpoint. For safety reasons, the rotor—bearings system was equipped with a lockable casing made of hard transparent plastic.

The rotor is supported by two hydrodynamic bearings with the same geometries. The radial bearing clearance is 76 μm and the bearing length is 12.6 mm. Every bearing has two supply ports located horizontally on both sides of the shaft. The supply ports have a diameter of 2.54 mm. The oil supply pressure was 0.16 MPa. The viscosity grade of the lubricating oil is consistent with the recommendations stated in ISO 13.

It should be stressed that dynamics of the rotating system is affected not only by the coupling and bearings but also by the whole supporting structure [13]. There are also some elements that have an impact on vibrations of the entire system since they influence vibration trajectories of the bearing journals [14].

3 Calculation Procedure

The movement of a point can be described using Eq. (1). After some transformations described in [6] it was possible to obtain the equation that can be used for calculating bearing dynamic coefficients (2), where ω denotes frequency.

$$m \cdot \ddot{x} + c \cdot \dot{x} + k \cdot x = f(t) \quad (1)$$

$$\begin{bmatrix} k_{xx} - m_{xx}\omega^2 + c_{xx}j\omega & k_{xy} - m_{xy}\omega^2 + c_{xy}j\omega \\ k_{yx} - m_{yx}\omega^2 + c_{yx}j\omega & k_{yy} - m_{yy}\omega^2 + c_{yy}j\omega \end{bmatrix} \cdot \begin{bmatrix} 1 & 0 & -\omega^2 & 0 & j\omega & 0 \\ 0 & 1 & 0 & -\omega^2 & 0 & j\omega \end{bmatrix} \\ = \begin{bmatrix} k_{xx} & k_{xy} \\ k_{yx} & k_{yy} \\ m_{xx} & m_{xy} \\ m_{yx} & m_{yy} \\ c_{xx} & c_{xy} \\ c_{yx} & c_{yy} \end{bmatrix} \quad (2)$$

During the experimental research that served for the determination of stiffness, damping and mass coefficients, forty-second periods of the rotor operation were registered. In each measurement, the rotor was excited in the Y direction a dozen or so times (using an impact hammer). Then the whole operation was repeated, but this time the rotor was excited in the direction perpendicular to its axis of rotation, namely, the X direction. For the calculation purposes, there was a need to obtain the signal fragments recorded from the time the excitation is applied and lasting until the rotor returns to its normal operating cycle. For each rotational speed tested, 10 signal fragments in the X and Y directions were chosen. The calculations were carried out for 11 rotational speeds in the range 2250–6000 rpm, making a total of 220 sets of measurement series. During each measurement series, four eddy current sensors served for measuring rotor vibrations. They recorded displacements in two mutually perpendicular directions, near each bearing support. In the calculation process, 220

signals recorded after the excitations were used and also the reference signals (registered with no excitations present). A proper preparation of data needed to compute the bearings' dynamic coefficients was very time-consuming.

During the preparation of data, for each signal registered after the excitation took place, its corresponding reference signal had to be subtracted from it. This was done for both bearings in one computational step. For each rotational speed tested, 10 sets of stiffness, damping and mass coefficients were determined. And then four sets that had the highest standard deviation values were rejected. On the basis of the remaining six sets, mean values and standard deviations of stiffness and damping coefficients were computed for each rotational speed.

4 Measurement Results

In order to obtain the complete set of data needed to compute the bearings' dynamic coefficients for one rotational speed, it was necessary to conduct the analysis in two stages. In the first stage, the rotor was excited in the Y direction using an impact hammer. In the second stage of the analysis, the rotor operated at the same speed and the impact hammer applied a force perpendicular to the Y direction, namely, the force acting in the X direction.

The determination of stiffness, damping and mass coefficients was performed simultaneously for two bearings. Bearing no. 1 is situated near the coupling that connects the rotor shaft with the drive motor's shaft, and bearing no. 2 is mounted on the opposite side of the test rig. Excitation forces were applied using an impact hammer that hit the shaft near the rotor disk located between the bearing supports. As it turns out, the coupling has a significant impact on the experimental results. In order to obtain reliable values of bearings' dynamic coefficients, this impact should be minimised in some way.

The plots illustrating the values of stiffness, damping and mass coefficients obtained for bearing no. 2 (situated far away from the coupling that heavily influences the rotor operation) are shown in Fig. 3. We can divide the results into two parts. Let the first part denote the results obtained for speeds in the range of 2250 to 3750 rpm and the second part the results obtained for speeds higher than 3750 rpm. This division can be defined on the basis of the size of vibration trajectories of the rotor. It can be observed that in the first speed range the vibration amplitudes are small. In the second speed range, the amplitudes are significantly higher than in the first range; moreover, a resonance occurs there. Looking at the plot that shows values of the stiffness coefficients of the hydrodynamic bearings, the same division can be applied. Let us note that the values obtained for speeds higher than 3750 rpm are characterised by higher standard deviations.

Let us also say a few words about graphs that demonstrate vibration spectra. It can be observed that the 1X component dominates on all graphs obtained for the bearing no. 2 and for speeds lower than 2750 rpm. For higher speeds, the 1/2X component is dominant. This is a clear indication of the hydrodynamic instability

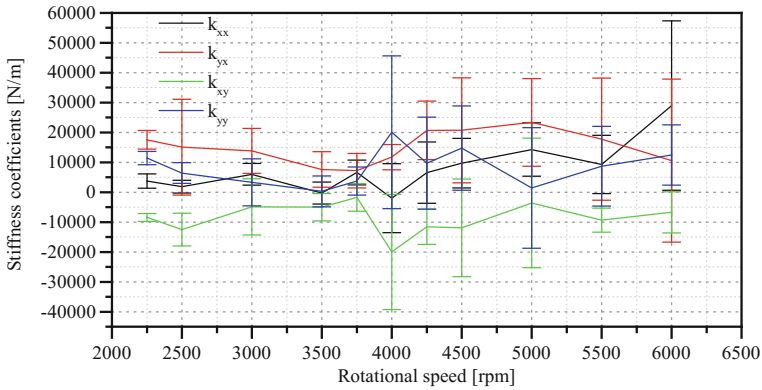


Fig. 3 The experimentally determined stiffness coefficients of bearing no. 2 versus rotational speed

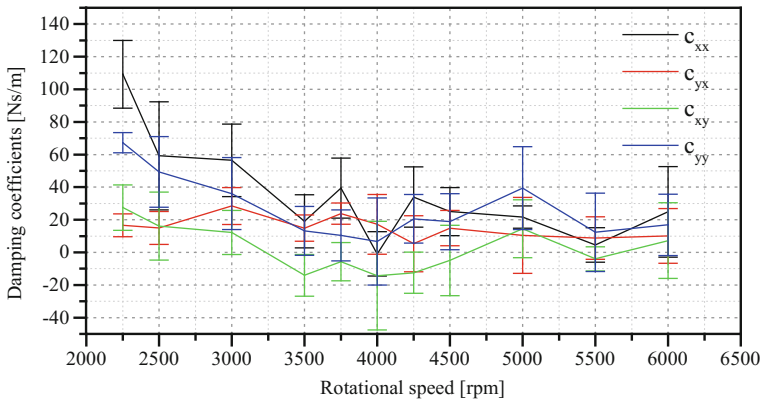


Fig. 4 The experimentally determined damping coefficients of bearing no. 2 versus rotational speed

and nonlinear properties of the bearings’ lubrication film. The phenomenon of the hydrodynamic instability may be caused by many reasons, such as an inappropriate geometry of the bearing (e.g. not carefully selected radial clearance or the skewed bush), an improper oil pressure, a change in the viscosity of the oil brought about by a change in its temperature or a whippy rotor.

Figure 4 presents values of the damping coefficients versus rotational speed. As can be seen, the damping coefficients decrease (coming close to zero) as the rotational speed increases. For a speed close to 4000 rpm, the c_{xy} coefficient takes a value lower than zero. It means that the vibrations that occurred after the excitation force was applied are not damped but their amplitude rises.

Figure 5 shows values of the mass coefficients of bearing no. 2 versus rotational speed. It is interesting to note that if we draw the curves representing m_{2XX} and m_{2YY} coefficients using the linear interpolation (in the form of a polynomial function of a low degree), one curve increases and the other one decreases. Moreover, they intersect

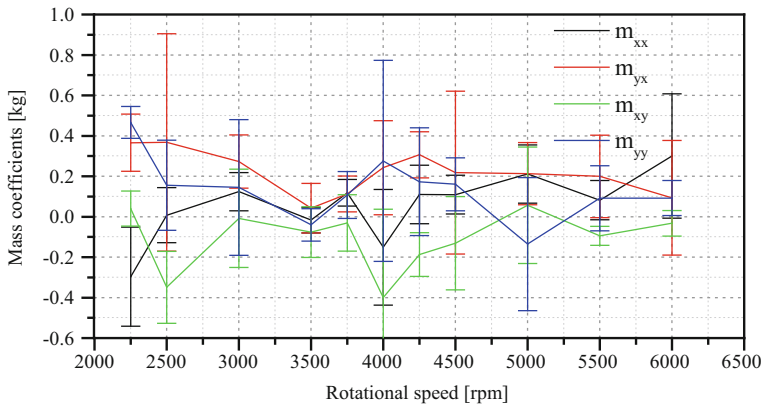


Fig. 5 The experimentally determined mass coefficients of bearing no. 2 versus rotational speed

and pass through zero at the speed at which the resonance occurs. The shaft mass calculated on the basis of the mass coefficients obtained at a speed of 2250 rpm can be described by the following formula:

$$m_{2xx} + m_{2yy} + m_{2xy} + m_{2yx} = (0.3 \pm 0.25) + (0.47 \pm 0.08) + (0.04 \pm 0.09) + (0.37 \pm 0.14) = 1.18 \pm 0.56 \text{ kg} \quad (3)$$

Comparing this value with a half of the mass of the shaft (i.e. 2.35 kg), it turns out that we get a result that is about two times lower than the real mass of the shaft.

At some rotational speeds, damping coefficients have values lower than zero, and this observation can be related to the resonance phenomenon. Figure 6 presents a signal registered at the second bearing during the operation at a speed of 4000 rpm after the excitation applied in the Y direction. It can be seen that the vibration amplitude increases from 0 to over $30 \mu\text{m}$ during a period of 300 ms. It means that the operation of the rotor is far from a stable operation and can even lead to a serious damage to the fluid-flow machine.

5 Verification of the Obtained Results

In order to verify the experimental results, a verification method proposed by Qiu and Tieu was used [5]. A model of the system that consists of a mass point with one degree of freedom, damping coefficients and stiffness coefficients was developed (using the Abaqus 6.14-2 software). The value of the force used during the experimental research and also the experimentally determined stiffness and damping coefficients were incorporated into the model. The model served to calculate the displacement of the mass point to which the impulse force was applied. The calculated displacement

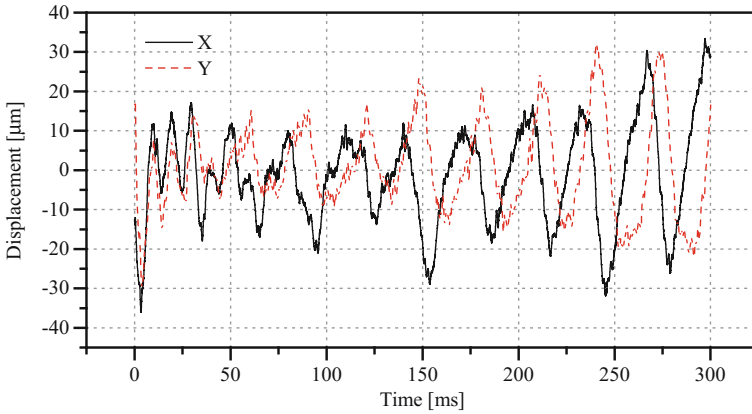
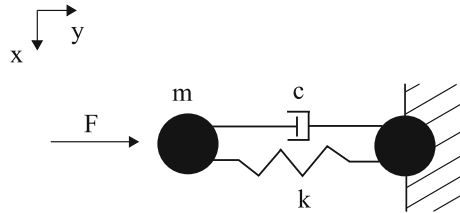


Fig. 6 Vibration amplitude registered at bearing no. 2 during the operation at a speed of 4000 rpm after an excitation was applied in the Y direction (using an impact hammer) versus time

Fig. 7 Schematic diagram of the model that consists of a concentrated mass, damping coefficients and stiffness coefficients



was then compared with the system response measured during the experimental research.

The model, created using the Abaqus, consists of two points lying on a straight line. The first point has all degrees of freedom removed and the second point has only one degree of freedom, namely, the displacement in the Y direction. The mass of the second point is 2.35 kg, which equals to a half of the mass of the rotor (measured during the experimental research). An element, characterised by elastic and damping properties, has been inserted between the two points in question. The values of stiffness and damping have been measured experimentally and they are 8700 Nm and 51 Nm/s, respectively. A schematic diagram representing the created model is demonstrated in Fig. 7.

The value of the excitation force that was incorporated into the model corresponds to a half of the value of the force measured during the experimental research. The values of this force (in Newtons) for the subsequent time steps are as follows: $F = [0, 0, 11, 59, 49, 44, 10, 0]$ N.

The time step during the numerical analysis was consistent with the sampling frequency in the experimental research. The duration of the excitation force was approximately 0.1 ms (the same as during experimental research). The movement of the rotor was calculated for a time of 1 s.

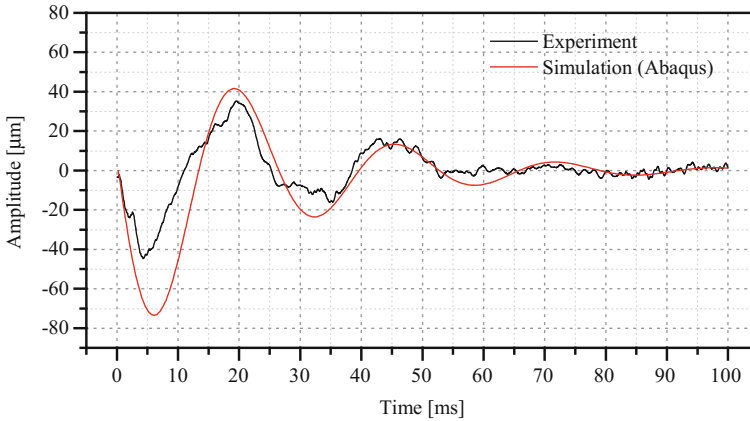


Fig. 8 The dynamic response of a real rotor and of its numerical model (into which the experimentally determined damping and stiffness coefficients were incorporated), presented as a function of time

The displacement of the point that has one degree of freedom is shown in 0The red line represents the results obtained using the model presented in this chapter of the article and the vibration amplitude measured during experimental tests is drawn using a black line. The results presented in Fig. 8 show that the stiffness and damping coefficients computed on the basis of the experimental research describe well the measured signals. Differences between experimentally and numerically obtained results can be explained by the presence of nonlinear damping in the system. Such a time-dependent damping is quite difficult to estimate as it has been proved in the paper [15].

6 Summary and Conclusions

On the basis of the research results, one can say that the values of the computed stiffness, damping and mass coefficients change in an expected manner in the whole speed range. The stiffness coefficients obtained for the lowest test speed (2250 rpm) are approximately 20,000 N/m. The highest stiffnesses bearing no. 2 were observed for coefficients: k_{xy} and k_{yx} . The values k_{xx} and k_{yy} are about twice lower. All stiffness coefficients decrease smoothly up to a speed of 3750 rpm and then rise around the resonant speed. The standard deviation values increase as the rotational speed of the rotor rises, which means that the calculated values are less repetitive.

The damping coefficients for bearing no. 2 take the highest values for low rotational speeds and they decrease as the speed increases. The value of c_{xx} coefficient oscillates around 110 Ns/m and the value of c_{yy} coefficient is about 65 Ns/m. The cross-coupled damping coefficients have values between 20 and 30 Ns/m. Almost

all obtained values of damping coefficients are higher than zero. Only around the resonant speed, c_{xy} coefficient is well below zero.

The mass coefficients computed for bearing no. 2 take the following values: m_{yy} and m_{yx} —approx. 0.4 kg, m_{xx} and m_{xy} —approx. -0.4 kg. It is interesting to note that if we draw the curves representing m_{xx} and m_{yy} coefficients using the linear interpolation (in the form of a polynomial function of a low degree), the values of these coefficients change from positive values (at low speeds) to approximately the same but negative values, at highest tested speeds. These curves pass through zero around the resonant speed. This is consistent with the fact that the ellipses representing the motion of the shaft rotate by some angle around the rotation axis of the shaft after passing through the resonant speed.

This article describes the computations of dynamic coefficients of hydrodynamic bearings carried out not only for a stably-operating machine but also for a broad range of rotational speeds. It turns out that the results obtained are less accurate at speeds at which higher vibration amplitudes are observed, which is reflected by increased standard deviation values. The method presented herein should be used only for analysing stably-operating rotating systems (i.e. systems that are characterised by small vibration amplitudes). Though the method allows computing dynamic coefficients of hydrodynamic bearings, damping coefficients obtained using impulse excitations can take negative values—this is due to an increased vibration amplitude after the excitation and the insufficient damping capability. The presented analysis is associated with an increased risk of obtaining inaccurate results and hence should be performed with a great caution. During passing through the resonant speed, mass coefficients can change from positive values to negative values (and vice versa).

Acknowledgements The research is being financed by the National Science Centre (NCN) in Poland under the research project no. 2015/17/N/ST8/01825. Calculations were carried out at the Academic Computer Centre in Gdańsk (CI TASK).

References

1. Tiwari, R., Lees, A.W., Friswell, M.I.: Identification of dynamic bearing parameters: a review. *Shock Vib. Dig.* **36**, 99–124 (2004)
2. Wang, X., Li, H., Meng, G.: Rotordynamic coefficients of a controllable magnetorheological fluid lubricated floating ring bearing. *Tribol. Int.* **114**, 1–14 (2017)
3. Li, Q., Wang, W., Weaver, B., Wood, H.: Model-based interpolation-iteration method for bearing coefficients identification of operating flexible rotor-bearing system. *Int. J. Mech. Sci.* **131–132**, 471–479 (2017)
4. Nordmann, R., Schoellhorn, K.: Identification of stiffness and damping coefficients of journal bearings by means of the impact method. In: 2nd International Conference on Vibrations in Rotating Machinery, pp. 231–238 (1980)
5. Qiu, Z.L., Tieu, A.K.: Identification of sixteen force coefficients of two journal bearings from impulse responses. *Wear* **212**, 206–212 (1997)
6. Breńkacz, Ł.: Identification of stiffness, damping and mass coefficients of rotor-bearing system using impulse response method. *J. Vibroeng.* **17**, 2272–2282 (2015)

7. Breńkacz, Ł., Żywica, G.: The sensitivity analysis of the method for identification of bearing dynamic coefficients. In: Awrejcewicz, J. (ed.) *Dynamical Systems: Modelling*: Łódź Poland, December 7–10, 2015, pp. 81–96. Springer International Publishing, Cham (2016)
8. Kudra, G., Awrejcewicz, J.: Application and experimental validation of new computational models of friction forces and rolling resistance. *Acta Mech.* **226**, 2831–2848 (2015)
9. Awrejcewicz, J., Dzyubak, L.P.: Chaos caused by hysteresis and saturation phenomenon in 2-DOF vibrations of the rotor supported by the magneto-hydrodynamic bearing. *Int. J. Bifurc. Chaos.* **21**, 2801 (2011)
10. Kaźmierczak, M., Kudra, G., Awrejcewicz, J., Wasilewski, G.: Mathematical modelling, numerical simulations and experimental verification of bifurcation dynamics of a pendulum driven by a dc motor. *Eur. J. Phys.* **36** (2015)
11. Breńkacz, Ł., Żywica, G.: An experimental investigation conducted in order to determine bearing dynamic coefficients of two hydrodynamic bearings using impulse responses. *Trans. Inst. Fluid-Flow Mach.* **133**, 39–54 (2016)
12. Breńkacz, Ł., Żywica, G., Drosińska-Komor, M.: The experimental identification of the dynamic coefficients of two hydrodynamic journal bearings operating at constant rotational speed and under nonlinear conditions. *Polish Marit. Res.* **24**, 108–115 (2017)
13. Bagiński, P., Żywica, G.: Analysis of dynamic compliance of the supporting structure for the prototype of organic Rankine cycle micro-turbine with a capacity of 100 kWe. *J. Vibroeng.* **18**, 3153–3163 (2016)
14. Jin, J., Wang, Z., Cao, L.: Numerical analysis on the influence of the twisted blade on the aerodynamic performance of turbine. *Pol. Marit. Res.* **23**, 86–90 (2016)
15. Olejnik, P., Awrejcewicz, J.: Coupled oscillators in identification of nonlinear damping of a real parametric pendulum. *Mech. Syst. Signal Process.* **98**, 91–107 (2018)